Pre-retrieval reperfusion decreases cancer recurrence after rat ischemic liver graft transplantation

Oldani, Graziano; Crowe, Lindsey A; Orci, Lorenzo; Slits, Florence; Rubbia-Brandt, Laura; De Vito, Claudio; Morel, Philippe; Mentha, Gilles; Berney, Thierry; Vallée, Jean-Paul; Lacotte, Stéphanie; Toso, Christian

How to cite

OLDANI, Graziano et al. Pre-retrieval reperfusion decreases cancer recurrence after rat ischemic liver graft transplantation. In: Journal of hepatology, 2014, vol. 61, n° 2, p. 278–285. doi: 10.1016/j.jhep.2014.03.036

This publication URL: https://archive-ouverte.unige.ch/unige:39093
Publication DOI: 10.1016/j.jhep.2014.03.036

Research Article

EASL EUROPEAN ASSOCIATION FOR THE STUDY OF THE LIVER | JOURNAL OF HEPATOLOGY

Pre-retrieval reperfusion decreases cancer recurrence after rat ischemic liver graft transplantation

Graziano Oldani[1,4], Lindsey A. Crowe[2], Lorenzo A. Orci[1], Florence Slits[1], Laura Rubbia-Brandt[3], Claudio de Vito[3], Philippe Morel[1], Gilles Mentha[1], Thierry Berney[1], Jean-Paul Vallée[2], Stéphanie Lacotte[1,†], Christian Toso[1,*,†]

[1]*Divisions of Transplant and Abdominal Surgery, Department of Surgery, Geneva University Hospitals and Faculty of Medicine, University of Geneva, Geneva, Switzerland;* [2]*Division of Radiology, Department of Medical Imaging, Geneva University Hospitals and Faculty of Medicine, University of Geneva, Geneva, Switzerland;* [3]*Division of Clinical Pathology, Geneva University Hospitals and Faculty of Medicine, University of Geneva, Geneva, Switzerland;* [4]*Department of Surgery, University of Pavia, Italy*

Transplantation

Background & Aims: Liver transplantation from marginal donors is associated with ischemia/reperfusion (I/R) lesions, which may increase the risk of post-transplant hepatocellular carcinoma (HCC) recurrence. Graft reperfusion prior to retrieval (as for extracorporeal membrane oxygenation – ECMO) can prevent I/R lesions. The impact of I/R on the risk of cancer recurrence was assessed on a syngeneic Fischer-rat liver transplantation model.

Methods: HCC cells were injected into the vena porta of all recipients at the end of an orthotopic liver transplantation (OLT). Control donors were standard heart-beating, ischemic ones (ISC), underwent 10 min or 30 min inflow liver clamping prior to retrieval, and ischemic/reperfused (ISC/R) donors underwent 2 h liver reperfusion after the clamping.

Results: I/R lesions were confirmed in the ISC group, with the presence of endothelial and hepatocyte injury, and increased liver function tests. These lesions were in part reversed by the 2 h reperfusion in the ISC/R group. HCC growth was higher in the 10 min and 30 min ISC recipients ($p = 0.018$ and 0.004 *vs.* control, as assessed by MRI difference between weeks one and two), and was prevented in the ISC/Rs ($p = 0.04$ and 0.01 *vs.* ISC). These observations were associated with a stronger pro-inflammatory cytokine profile in the ISC recipients only, and the expression of hypoxia and HCC growth-enhancer genes, including *Hmox1*, *Hif1a* and *Serpine1*.

Conclusions: This experiment suggests that ischemia/reperfusion lesions lead to an increased risk of post-transplant HCC recurrence and growth. This observation can be reversed by graft reperfusion prior to retrieval.

Keywords: Hepatocellular; Carcinoma; Donation after cardiac death; Extracorporeal membrane oxygenation.

Received 28 March 2013; received in revised form 28 February 2014; accepted 27 March 2014; available online 5 April 2014

* Corresponding author. Address: Department of Surgery, Rue Gabrielle-Perret-Gentil, 1211 Geneva, Switzerland. Tel.: +41 22 3723311; fax: +41 22 3727755.
E-mail address: christian.toso@hcuge.ch (C. Toso).

† These authors contributed equally to this work.

Abbreviations: DCD, donation-after-cardiac-death; I/R, ischemia/reperfusion; HCC, hepatocellular carcinoma; ECMO, extracorporeal membrane oxygenation; ISC, Ischemic; ISC/R, ischemic/reperfused; MELD, model of end-stage liver disease; SHVC, Supra-hepatic vena cava; MRI, Magnetic Resonance Imaging; D, dimension; TSE, turbo spin echo; UTE, ultrashort echo time; FA, flip angle; TE, echo time; TR, repetition time; IL, interleukin; TNF, tumor necrosis factor; VEGF, vascular growth factor; AST, aspartate aminotransferase; ALT, alanine aminotransferase; PCR, polymerase chain reaction; PBS, phosphate buffered saline.

Introduction

Liver transplantation is the best treatment for patients with end-stage liver failure and/or unresectable hepatocellular carcinoma (HCC). Its main limitation is the lack of donors, which faces an ever growing demand. While split- and living-liver donors only account for a small proportion of organ donation in most Western countries, the use of extended criteria grafts has become more liberal. Among them, donation-after-cardiac-death (DCD) donors (for whom death is declared by cardiac arrest rather than brain function cessation) have been considered as a promising source of organs, and DCD liver transplantations now represent some 10–15% of all liver transplantations in a number of centers [1–5].

DCD liver transplantations have shown acceptable post-transplant survival (65–80% at five years), similar to those achieved with transplantations from brain-dead donors [2–4]. However, these liver grafts are by nature subject to warm ischemia and ischemia/reperfusion (I/R) injury, leading to increased risks of primary non-function and late ischemic biliary lesions. In order to avoid combining marginal donors and marginal recipients, DCD transplantations tend to be more frequently offered to patients with a lower model for end-stage liver disease (MELD) scores, and especially to those with HCC [5]. This observation may represent a point of concern as I/R lesions have been shown to increase the risk of liver metastasis in various rodent models, due to the presence of endothelial lesions and increased growth signals [6,7]. Along the same line, post-transplant HCC recurrence is due to the presence of circulating HCC cells, released prior to or at the time of transplantation

and subsequently implanting in the liver graft [8]. One can therefore hypothesize that the ischemia/reperfusion injury occurring after transplantation of a marginal liver also alters the risk of post-transplant HCC recurrence.

The present study is assessing the impact of ischemic liver graft on the risk of cancer recurrence utilizing a rat liver transplantation model. The involved mechanisms are explored, as well as the potential to reverse the observed effect with the use of *in vivo* normothermic graft preconditioning.

Materials and methods

Animals

Experiments were performed on male Fischer (F344) rats (Charles River, France), both donors and recipients weighing 180–220 g. Animals were housed under 12/12-h light/dark cycles, with free access to food (standard diet) and water. The study was conducted under experimental protocols approved by the ethical committee of the University of Geneva and by the Geneva veterinary authorities.

Study design

Syngeneic Fisher-to-Fisher orthotopic liver transplantations were performed [9,10], with the injection of Fisher-derived JM-1 HCC cells into the portal vein at the end of the procedure. Donors were grouped as follow: non-ischemic (controls), ischemic (ISC), and ischemic/reperfused (ISC/R). Livers from ISC donors underwent a 10- or 30-min normothermic ischemia, by clamping the liver pedicle and the infra-hepatic vena cava prior to retrieval. The ischemic/reperfused donors had a two-hour *in vivo* reperfusion after the clamping, which approximates the extracorporeal machine oxygenation (ECMO) used for graft salvage after uncontrolled donation [4].

Surgical procedure

Rat liver retrieval and transplantation were performed under 2% isoflurane anesthesia, following a technique described previously [9]. Donor surgery: after ligating and transecting the collateral liver veins and the hepatic artery, the liver was flushed at low pressure with 150 U heparin diluted in 15 ml Ringer's solution through the vena porta, and retrieved. Ten units of heparin (in 1 ml NaCl 0.9%) were administered through the dorsal penile vein before flush and retrieval in all groups. Intermediate steps were introduced in the ISC and ISC/R groups. In the ISC group, the vena porta and infra-hepatic vena cava (IVC) were clamped during 10 or 30 min prior to flushing and retrieving the liver. In the ISC/R group, all clamps were removed at the end of the clamping, and the liver was reperfused *in vivo* (animal alive) for two hours prior to flushing and retrieving (hepatic artery being ligated and divided just before flushing). Immersed in 4 °C Ringer's solution, the liver graft was prepared for implantation by attaching cuffs to the IVC and the vena porta. The caudate lobe was removed by ligating its pedicle for subsequent analysis (liver graft biopsy). The recipient was prepared in parallel by another operator, assuring a constant graft cold ischemia time of 50 ± 10 min.

Recipient surgery: the abdomen was opened through a midline incision, the liver was freed from its ligamentous attachments and all liver vessels were isolated. Handling rings were attached to the infra-hepatic vena cava and the portal vein with four 9–0 Prolene (Ethicon Inc., New Brunswick, NJ) sutures. After intra-venous (iv) administration of 10 U of heparin (in 100 µl NaCl 0.9%) through the dorsal penile vein, clamps were applied to the IVC, the vena porta and the supra-hepatic vena cava (SHVC). The liver was explanted. The SHVC anastomosis was performed by hand with 8–0 Prolene running suture. The remaining anastomoses were performed using the quick-linker technique, allowing short implantation times [10]. After unclamping, the papillary process lobe was removed (reperfusion biopsy) and the bile duct continuity was established over a 4 mm polyethylene 26 gauge stent. The abdomen was closed in two layers with 5–0 Prolene running sutures. In a second set of experiments looking at the involved mechanisms, recipients were sacrificed on day one.

HCC cell injection

JM-1 cells have been kindly provided by Dr G. Michalopoulos (Duke University Medical Center, Durham, NC) [11]. Cells were grown and maintained in Dulbecco's modified Eagle medium (Gibco, Paisley, UK) in a 5% CO_2 atmosphere. At the end of the transplantation, $2 * 10^6$ (in the 10 min-ischemia rats) or $5 * 10^5$ (in the 30 min-ischemia rats) JM-1 cells suspended in 600 µl NaCl 0.9% were injected into the portal vein using a 25 G needle. Post-injection hemostasis was achieved with 9–0 Prolene suture around the hole.

Magnetic resonance imaging-based HCC volume assessment

Magnetic Resonance Imaging (MRI) was performed at weeks one and two on a Siemens Magnetom Trio 3 Tesla clinical scanner (a TIM system, Siemens AG, Erlangen, Germany) using the system wrist coil. With the animal placed prone in this volume coil, homogenous signal-to-noise ratio is obtained over the whole liver and abdomen. During imaging, animals were anesthetized by inhaled 2–3% isoflurane. Respiratory monitoring and triggering used a pressure pad system (SA Instruments Inc., USA).

After a standard fast localisation scan, two image sets were acquired, to give a combination of high resolution in 3-dimensions (3D) and two different contrast regimes to positively identify liver tumours from other structures such as normal liver and fluid collections. MRI acquisitions included a classical 2D T2-weighted turbo spin echo (TSE) and an ultrashort echo time (UTE) 3D isotropic acquisition that allow accurate quantification of 3D volumes of irregular shaped masses from multiple seed points.

The high contrast, T2-weighted 2D-TSE (turbo spin echo) sequence (TE/TR/FA = 57 ms/3500 ms/180°, 3 signal averages, 6 min acquisition time) was acquired with 0.3 mm pixel resolution, but with a minimum 1 mm slice thickness. This conventional sequence was more susceptible to motion artefacts and it was also non-triggered (due to the long TR), but gave high contrast for confirming the structures observed and subsequently segmented in the 3D UTE images. The long TR also means that 3D acquisition using T2 weighted TSE is not possible due to restrictively long acquisition times. The UTE sequence comprises a non-selective RF pulse and 3D radial acquisition to provide true 3D images, allowing post-processing reconstruction of any plane, with very low sensitivity to motion artefacts. The parameters were a 3D isotropic resolution 0.35 mm (in-plane and slice thickness), 11 cm FOV, 50000 radial projections, echo time TE 0.07 ms, repetition time TR 9.6 ms with up to 100 lines of data acquired per respiratory cycle, a 12° flip angle (FA) and an acquisition time of 8 min.

The high resolution (0.35 mm) allows volumes to be calculated in 3D. Software, Osirix (University of Geneva, available under open source licensing http://www.osirix-viewer.com/) was used for visualisation and comparison of image contrast, and a tool built by Paracelsus Medical University (Salzburg, Austria; F Eckstein, W Wirth) was used for semi-automatic segmentation and volume quantification of regions of interest seen on the MR images. Each tumor region is segmented based on pixel intensity as a single click in each 2D image slice fills the neighboring pixels within an intensity threshold. The total volume can then be calculated automatically in 3D by multiplying the number of pixels in all image slices by the pixel volume, finally expressed in mm^3. The change in volume between the two imaging sessions was assessed.

Serum cytokine and liver function test quantification

Tail vein serum cytokine levels were assessed using a Rat Fluorokine MAP Base Kit Luminex Performance Assay cytokine kit with interleukin (IL)-1β, IL-6, IL-10, tumor necrosis factor (TNF)α and vascular growth factor (VEGF) individual bead sets, according to the manufacturer's protocol (R&D Systems, MN, USA). Briefly, antibody-coated cytokine-specific beads were prepared in 96-well plates. Sera (diluted 1/4) were added to the wells for a 3-h incubation at room temperature in the dark with a 500 Hz shaking, allowing cytokines to bind to the cytokine-specific beads. Plates were subsequently washed and incubated with biotinylated anti-cytokine detection antibody for 60 min. After washing, streptavidin-PE was added for 30 min to bind to the detection antibody. The level of fluorescence of the cytokine-specific beads was analyzed by a double-laser Bio-Plex200 reader (BioRad, CA, USA). Cytokine concentrations were determined based on a standard curve included in each plate, using cytokine standards provided by the manufacturer.

Serum serotonin levels were assessed utilizing an ELISA kit (LDN GmbH& Co.KG, Nordhorn), according to the manufacturer's protocol. Liver function tests, including aspartate aminotransferase (AST), alanine aminotransferase (ALT), and

bilirubin, were quantified on day one after reperfusion in collaboration with the central clinical hospital laboratory (Synchron LX20, Beckman Coulter, Fullerton, CA).

Electron and light microscopy

For electron microscopy, liver samples were fixed with a 2.5% glutaraldehyde solution in 0.1 M phosphate buffer (pH 7.4), postfixed in 1% osmium tetroxide in the same buffer, dehydrated, and embedded in Epon. Ultrathin sections were examined and photographed with a Philips CM10 electron microscope.

For light microscopy, liver sections were stained with hematoxylin and eosin (Sigma, Buchs, Switzerland). Histological studies were performed blindly by an expert in liver anatomo-pathology.

Detection of proliferation by immunofluorescence

Liver section fixed in formol were treated with TEG Buffer (Tris base EGTA Buffer), washed (phosphate buffered saline: PBS), permeabilised (PBS-0.5% Triton X-100), rinsed (PBS), and satured (PBS-0.5% bovine serum albumin). They were then incubated with mouse anti-Ki-67 (BD Pharmingen, Basel, Switzerland) for 2 h (room temperature). Staining was detected using Alexa-fluor 488-conjugated goat anti-mouse Ig (Invitrogen, Carlsbad, CA). Nuclei were stained with 1 μg/ml Hoechst (Sigma-Aldrich, Buchs, Switzerland). The percentage of Ki67-cells in the total cells (Hoechst nuclear staining) was assessed in one to two HCC lesions per animal using Metamorph Software (40× magnification).

Real-time polymerase chain reaction (PCR)

PCR assessments were performed on 12-h liver samples. Total RNA was prepared and purified from frozen-crushed liver powder using the RNeasy Mini Kit (Qiagen, Germantown, MD), and according to the manufacturer's instructions. One μg of cDNA was synthesized by extending a mix of random primers with the High Capacity cDNA Reverse Transcription Kit in the presence of RNase Inhibitor (Applied Biosystems, Carlsbad, CA). The relative quantity of each transcript was normalized according to the expression of *rplp1* (ribosomal protein large P1). Primer sequence for *rplp1*, *htr2a*, and *htr2b* (forward/reverse) were designed with the Primers3 software (http://packages.debian.org/fr/sid/primer3) and are available upon request. Amplification reactions were performed in a total volume of 20 μl using a Thermocycler sequence detector (BioRad CFX96) with qPCR Core kit for SYBR Green I (Eurogentec, Seraing, Belgium).

The "Rat Endothelial Cell Biology" RT2 Profiler PCR Array (SaBiosciences, Frederick, MD) was first used according to manufacturers' instructions. Specific PCR assessments were subsequently performed for genes of interest selected among those with a fold increase/decrease between ISC and ISC/R animals $\geqslant$1.8 in the array, and because of their known or expected involvement in ischemia-reperfusion and/or in HCC growth. Of note, genes with high (>35) cycle threshold were excluded. Selected genes included *Casp3* (caspase 3), *Fas* (Fas cell surface death receptor), *Fn1* (fibronectin 1), *Flt1* (FMS-related tyrosine kinase 1), *Hif1a* (hypoxia-inducible factor 1), *Hmox1* (heme oxygenase (decycling) 1), *Icam1* (intercellular adhesion molecule 1), *Serpine1* (plasminogen activator inhibitor type 1), and *Vwf* (von Willebrand factor) (Quiagen, Hilden, Germany).

Statistical analysis

Data were expressed as median [min-max] and were analyzed using Prism 6 (GraphPad Software Inc., CA, USA). Continuous variables were compared using the Wilcoxon test, when referring to the same animals at different time-points, and the Mann-Whitney test when comparing different groups. The limit for statistical significance was set at $p = 0.05$.

Results

Validation of the ischemia/reperfusion rat liver transplantation model

In an effort to validate the ISC rat liver transplantation model, the presence of ischemia/reperfusion lesions was assessed. Macroscopically, liver grafts demonstrated patchy dark surface areas, when retrieved after 10 and 30 min of ischemia (ISC group). These lesions were reversed after the two-hour reperfusion (ISC/R group, Fig. 1A). Microscopically, control liver grafts demonstrated normal architectures, with only minimal (<5% of hepatocytes) centro-lobular micro-vacuolar steatosis. ISC and ISC/R liver grafts (10- and 30-min ischemia) showed more frequent lesions of hepatocyte injury with more micro-vacuolar steatosis (up to 30%) and rare apoptotic bodies associated with inflammatory infiltrates (Fig. 1A). Of note, the 30-min ISC and ISC/R grafts tended to demonstrate less steatosis than the 10-min grafts, probably reflecting a more advanced stage of ischemia.

On day one after transplantation, most micro-vacuolar steatosis lesions had disappeared (minimal <1% lesions remained) on standard microscopy, and control livers only demonstrated isolated apoptotic bodies. By contrast, ISC and ISC/R recipients (10- and 30-min ischemia) showed more signs of hepatocyte injury, with mild focal aggregates of apoptotic bodies (Fig. 1B). In addition, 30-min ISC and ISC/R recipients also demonstrated large areas of centro-lobular necrosis (Fig. 1C).

On electronic microscopy, the 12-h liver graft endothelial cells demonstrated a normal appearance in the control group. By contrast, the ISC and ISC/R recipients showed signs of endothelial injury with ballooning and apoptotic cells (Fig. 1B).

As a whole, day-one AST serum assessment confirmed a greater level of cytolysis in ISC recipients compared to controls and ISC/R (10-min ischemia experiments: 1898 [380–6741], 740 [213–2505], and 1155 [245–2405] U/L respectively; ISC *vs.* control $p = 0.009$, ISC *vs.* ISC/R $p = 0.117$; and 30-min ischemia experiments: 9524 [1930–29762], 2510 [1090–6324], and 6012 [1010–10660] U/L respectively; ISC *vs.* control $p = 0.021$, ISC *vs.* ISC/R $p = 0.085$). ALTs demonstrated similar trends with higher levels in ISCs, compared to controls and ISC/Rs (10-min ischemia experiments: ISC 893 [80–3870], 430 [80–1500], ISC/R 463 [20–2480] U/L; ISC *vs.* control $p = 0.10$, ISC *vs.* ISC/R $p = 0.30$, and 30-min ischemia experiments: ISC 6149 [1390–18850], 1995 [710–4893], ISC/R 3954 [630–7690] U/L; ISC *vs.* control $p = 0.028$, ISC *vs.* ISC/R $p = 0.69$). Bilirubin levels were similar between groups.

Increased MRI-assessed HCC growth in ischemic liver graft (ISC) recipients

All injected animals developed MRI-detectable HCCs one week after transplantation (Fig. 2A and B). Week-two MRI assessments demonstrated a significant increase in the ISC HCC volumes (10-min ischemia experiments: 838 [192–4225] mm^3 *vs.* 4758 [1386–15,741] mm^3 $p = 0.0008$; and 30-min ischemia experiments: 1400 [469–2064] mm^3 *vs.* 6298 [3403–9526] mm^3 $p = 0.004$). As a result, the MRI-assessed HCC growth between week one and week two was significantly higher in the ISC group compared to the other two (10-min ischemia experiments: ISC *vs.* controls $p = 0.018$ and ISC *vs.* ISC/R $p = 0.04$; and 30-min ischemia experiments: ISC *vs.* controls $p = 0.004$ and ISC *vs.* ISC/R $p = 0.010$, Fig. 2C and D). There was no growth difference between the control and the ISC/R groups ($p = 0.74$ and $p = 0.81$).

On standard histology, tumors had similar patterns in all animals, demonstrating signs of an aggressive poorly differentiated malignant lesion, with numerous mitosis, high nucleo-cytoplasmic ratio and irregular chromatin. Focal areas of tumor necrosis were observed. In addition, most cells were of epithelioid type, but some lesions also showed areas with fusiform cells, another

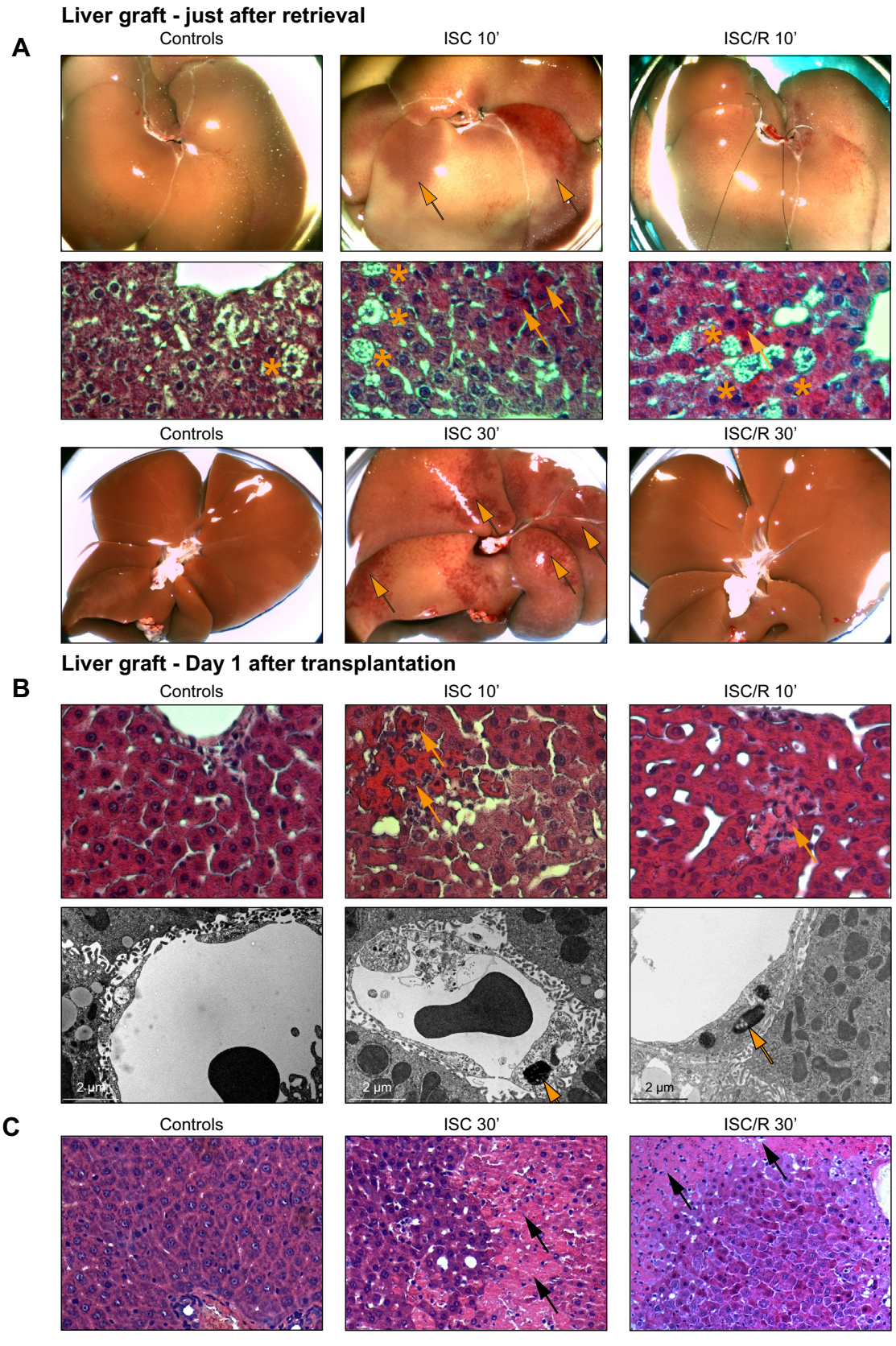
Liver graft - just after retrieval
A
Controls
ISC 10'
ISC/R 10'
Controls
ISC 30'
ISC/R 30'
Liver graft - Day 1 after transplantation
B
Controls
ISC 10'
ISC/R 10'
2 µm
2 µm
2 µm
C
Controls
ISC 30'
ISC/R 30'

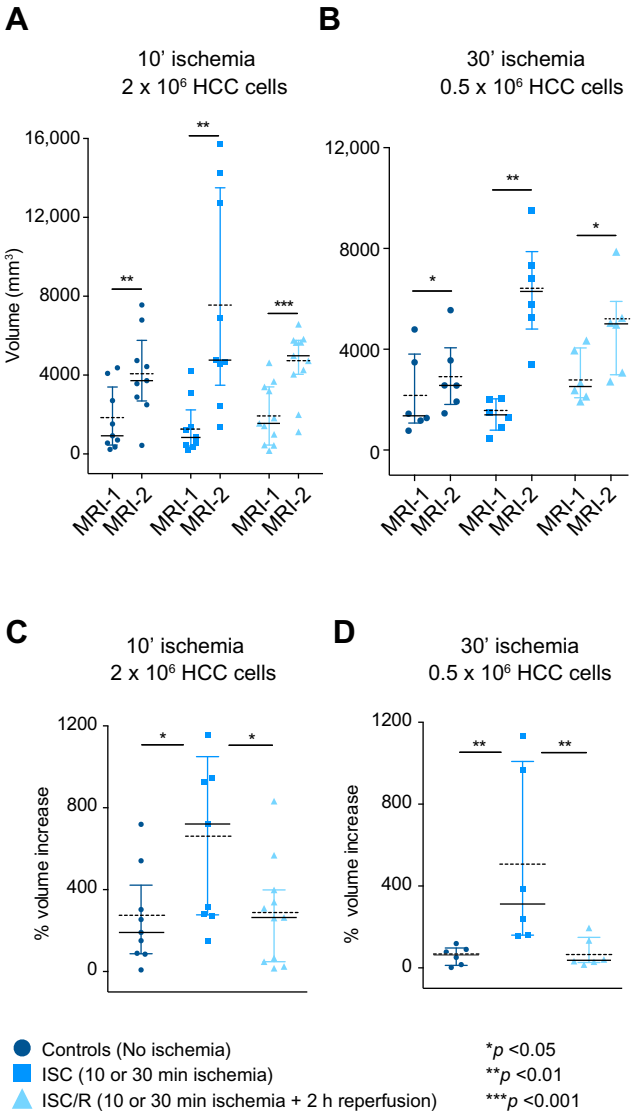

Fig. 2. HCC growth and proliferation after transplantation. (A, B) Tumor volume (mm^3) assessed by MRI at one and two weeks after transplantation. (C, D) MRI-assessed HCC growth (% of volume increase) between week one and week two after transplantation. (This figure appears in colour on the web.)

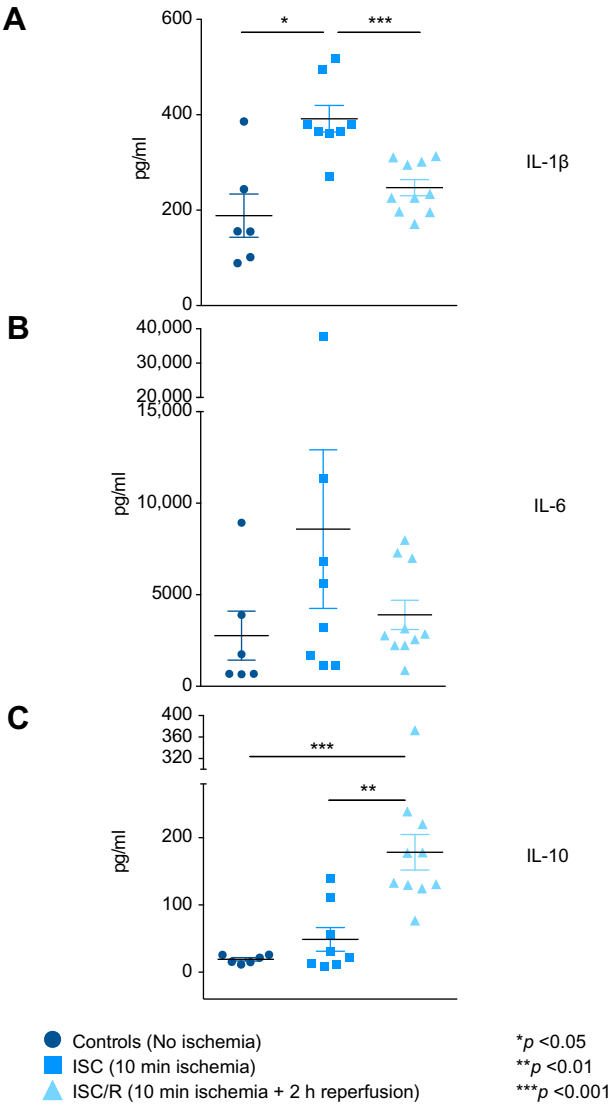

Fig. 3. Cytokine profile analysis after transplantation. Post-transplantation (12 h) serum concentration of rat IL-1β (A), IL-6 (B), and IL-10 (C), assessed using Bioplex assay (pg/ml) in the 10-min experiments. Median: full line, mean: dashed line. (This figure appears in colour on the web.)

sign of aggressiveness. None of the animals developed spleen or lung metastasis (only about 1 mm peritoneal nodules were detected at the injection site in most animals).

In parallel to the MRI-assessed HCC growth, ISC recipients also tended to have higher levels of cancer cell proliferation in the 10-min ischemia experiments. Two weeks after transplantation, 42 [34–59]% of the cancer cells were Ki67 positive in the ISCs *vs.* 40 [27–55]% in the controls ($p = 0.12$) and 34 [18–57]% in the ISC/Rs ($p = 0.013$).

Increased HCC growth/proliferation and serotonine and VEGF levels

Because serotonin has been suggested as an important mediator of normal hepatocyte and HCC cell proliferation, serotonin and its

Fig. 1. Validation of the ischemia/reperfusion (I/R) injury rat liver transplantation model. (A) Representative pictures of liver grafts in the three groups. Arrows indicate patchy dark surface areas. H&E stained sections of just retrieved liver grafts in the three groups. Arrows indicate apoptotic bodies and stars microsteatosis, both predominant in rats subjected to 10 min warm ischemia before retrieval (ISC) and in those experiencing 2 h *in vivo* reperfusion, after 10 min warm ischemia, before retrieval (ISC/R). (B) H&E stained sections of liver grafts twelve hours after transplantation. Arrows show focal aggregates of apoptotic bodies. Electron microscopy sections of liver grafts twelve hours after transplantation. Arrows show apoptotic endothelial nuclei in ISCs and ISC/Rs, while grafts from the control group appear uninjured. (C) H&E stained sections of liver grafts on day one after transplantation show large areas of necrosis (arrow) in rats subjected to 30 min warm ischemia before retrieval (ISC) and in those experiencing 2 h *in vivo* reperfusion, after the 30 min warm ischemia (ISC/R).

receptors were assessed [12,13]. The 12-h serum serotonin levels were similar between groups in the 10-min ischemia experiment (controls 22 [14–46] ng/ml, ISC 19 [14–28] ng/ml, ISC/R 30 [22–36] ng/ml, ISC *vs.* control $p = 0.62$, ISC *vs.* ISC/R $p = 0.11$ and ISC/R *vs.* control $p = 0.37$). In addition, the levels of expression of the serotonin receptors *htr2a* and *htr2b* were also similar between groups (data not shown).

At 12 h, VEGF serum levels, *VEGF* and *Flt1* (tyrosine kinase receptor for vascular endothelial growth factor) liver expressions were also similar between groups (data not shown).

Increased serum inflammatory profile in the ischemic liver graft (ISC) recipients

ISC recipients demonstrated a stronger pro-inflammatory serum cytokine profile 12 h after transplantation in the 10-min experiment. IL1β was higher in ISCs (372 [271–517] pg/ml) *vs.* controls (155 [102–385] pg/ml) and ISC/Rs (234 [171–313] pg/ml; ISC *vs.* control $p = 0.020$, ISC *vs.* ISC/R $p = 0.0005$, ISC/R *vs.* control $p = 0.14$, Fig. 3A). IL6 also tended to be higher in ISC and ISC/R recipients, but did not reach statistical significance (Fig. 3B). By contrast, IL10 was higher in the ISC/R group, suggesting an anti-inflammatory effect of this treatment (ISC/R 177 [77–372] pg/ml, controls 18 [11–26] pg/ml, and ISC 25 [9–138] pg/ml; ISC *vs.* control $p = 0.51$, ISC *vs.* ISC/R $p = 0.0014$, ISC/R *vs.* control $p = 0.0002$, Fig. 3C). TNF-α was undetectable in the serum of all groups 12 h after transplantation.

Decreased expression of liver injury genes in the ischemic/reperfused liver graft (ISC/R) recipients

The level of expression was first tested using the "Rat Endothelial Cell Biology" RT2 Profiler PCR Array (SaBiosciences, Frederick, MD) (Supplementary Fig. 1), and subsequent specific PCR assessments were performed for selected genes in the 10-min experiments. *Hmox1*, *Hif1a*, and *Serpine1* (plasminogen activator inhibitor-1), have been previously shown to be up-regulated in case of liver hypoxia and injury [14–16]. The levels of these genes were lower in the ISC/R recipient grafts 12 h after transplantation (Fig. 4A–C). *Hmox1* level was 0.41 [0.31–0.87] in the ISC/R *vs.* 1.23 [0.70–3.03] in the controls and 2.51 [0.53–7.26] in the ISC (ISC/R *vs.* controls $p = 0.0006$, ISC/R *vs.* ISC $p < 0.0001$). *Hif1a* level was 0.65 [0.45–0.78] in the ISC/R *vs.* 0.89 [0.75–1.38] in the controls and 1.03 [0.90–1.56] in the ISC (ISC/R *vs.* controls $p = 0.0048$, ISC/R *vs.* ISC $p < 0.0001$). *Serpine1* level was 0.25 [0.1–2.71] in the ISC/R *vs.* 0.84 [0.55–5.92] in the controls and 2.06 [0.28–5.41] in the ISC (ISC/R *vs.* controls $p = 0.058$, ISC/R *vs.* ISC $p = 0.0011$). The other tested genes, including *Casp3*, *Fas*, *Fn1*, *Flt1*, *Icam1*, and *Vwf* demonstrated similar levels between groups.

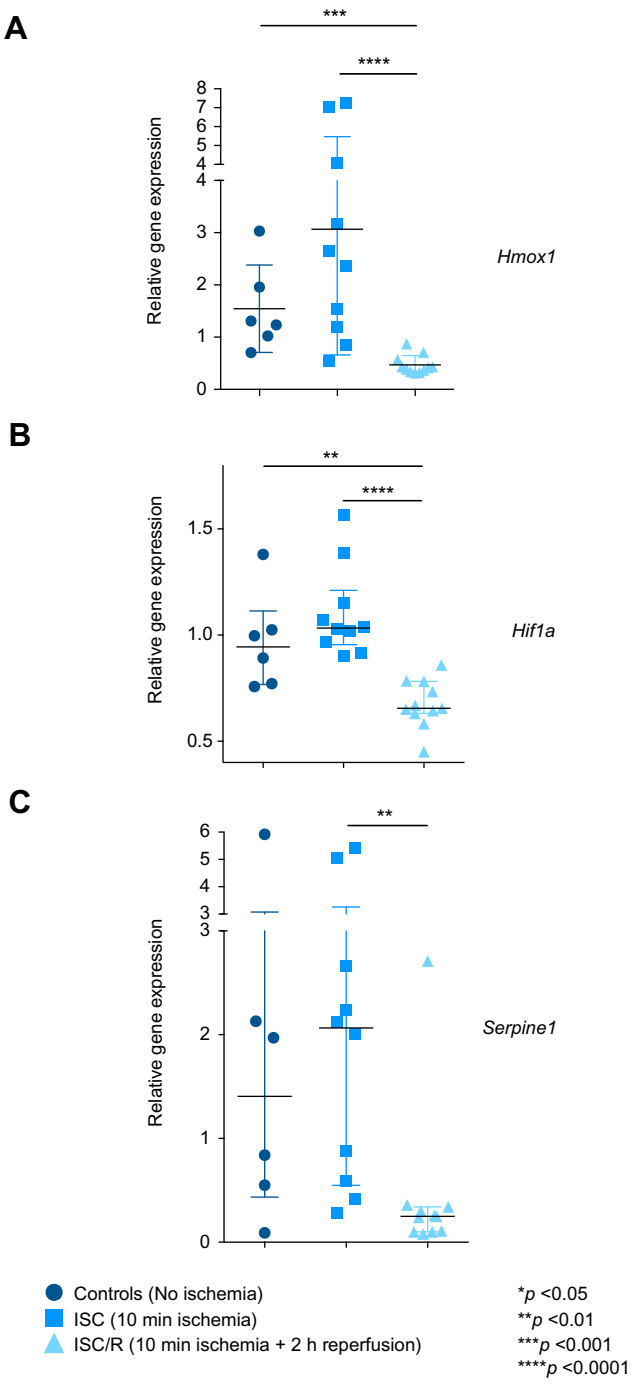

Fig. 4. Gene profile analysis after transplantation. Post-transplantation (12 h) gene expression profile, assessed by qPCR on RNA extracted from liver parenchyma. Relative gene expression of heme oxygenase decycling 1 (*Hmox1*) (A), hypoxia-inducible factor 1 (*Hif1a*) (B) and plasminogen activator inhibitor type 1 (*Serpine1*) (C) was evaluated in the three groups in the 10-min experiments and normalized according to the expression of the housekeeping gene *rplp1*. Median: full line, mean: dashed line. (This figure appears in colour on the web.)

Discussion

The present study demonstrates that the use of ischemic rat liver graft increases HCC growth after transplantation, and that this observation is reversed by a normothermic graft reperfusion prior to retrieval.

In the used ISC model, liver ischemia was induced by a 10- or 30-min total liver clamping prior to retrieval. It induced significant liver lesions, including hepatocyte (micro-vacuolar steatosis, apoptotic bodies, increased liver function tests) and endothelial (ballooning and apoptosis) injury. The ISC recipients demonstrated increased HCC total volume two weeks after transplantation, with higher MRI-assessed HCC growth rates and more numerous Ki67-stained proliferating HCC cells.

DCD donors are an increasingly used source of liver grafts and an intense field of investigation [1–5]. Most studies are aiming at reversing the cardiac arrest-induced ischemia/reperfusion injury and improving the overall graft quality. Among others, investigators have looked at the use of *ex vivo* hypothermic oxygenated graft perfusion [19–21] and *ex vivo* [17,18] or *in vivo* (ECMO) normothermic perfusion [22]. While the debate is not fully closed regarding the pros and cons of these techniques, we have chosen a model which approximates an *in vivo* normothermic perfusion. In the present experiment, the treatment did not reverse the already constituted apoptotic and necrotic hepatocyte and endothelial lesions (similarly observed in the ISC and ISC/R groups). However, it decreased the overall level of injury, with lower levels of liver function tests. In addition, prior-to-retrieval reperfusion was associated with lower MRI-assessed HCC growth rates and less Ki67-stained proliferating hepatocytes compared to the ISC recipients.

The observed increased post-transplant HCC volumes in the ISC recipients and their prevention by reperfusion prior to retrieval are associated with a number of studied mechanisms (the present data do not provide a causal relationship). First, the 12-h expression of a panel of ischemia-related genes, including *Hmox1*, *Hif1a*, and *Serpine1* was decreased in the ISC/R group. *Hmox1* is coding for heme oxygenase 1, an inducible isoform of heme oxygenase in response to stress. Inhibition of Hmox1 by molecules or small interfering RNA prevents the *in vitro* HCC cell migration and proliferation, and the *in vivo* HCC growth, by shifting the endogenous balance between apoptosis and proliferation towards an anti-proliferative status [23–25]. *Hif1a* is coding for the hypoxia-inducible factor 1, which is essential in the cellular and systemic response to hypoxia. Its expression is increased in HCC, and it is associated with worse clinical outcomes [26]. Hypoxia-inducible factor 1 inhibition decreased cancer growth in a murine model [27]. *Serpine1* is coding for the plasminogen activator inhibitor-1, which inhibits plasmin action and impairs matrix degradation. It has been identified as a factor contributing to the development of HCC [28]. The presence of an increased serum pro-inflammatory cytokine profile in the ISC recipients may also contribute to HCC growth. IL1, TNFα and IL6 have been shown to regulate cancer promotion, growth, and invasiveness [29,30]. By contrast, the presence of IL10 in the ISC/R recipients reflects a more anti-inflammatory cytokine profile in this group. Finally, the liver endothelial cell lesions (ballooning, apoptosis) observed on electronic microscopy may also play a role, by enhancing cell adhesion and migration, and angiogenesis pathways [31,32].

Of note, the observed post-transplant HCC growth appeared independent of serotonin and VEGF, both important factors in the normal hepatocyte and HCC growth. These analyses were conducted 12 h after transplantation, and an earlier or later increase in the serum protein level or in the gene liver expression could have been missed.

The clinical relevance of these rat observations remains to be fully determined. The used model only approximates the clinical features of ischemia/reperfusion and marginal liver graft preconditioning. In addition, a large number of HCC cells was injected into the portal vein, and this cell concentration is likely higher than the one present in the blood stream during transplantation for HCC. However, some investigations suggest that DCD liver transplantation may be related to increased death after transplantation for HCC [33]. Altogether the use of a (re)perfusion protocol for DCD and marginal liver graft pre-conditioning deserves further clinical exploration.

The present data demonstrates an increased risk of HCC recurrence and growth after transplantation of ischemic rat liver graft, and its prevention with use of graft reperfusion prior to retrieval. These observations were associated with alterations in the inflammatory cytokine profile and in the expression of various genes, including *Hmox1*, *Hif1a*, and *Serpine1*.

Financial support

This study was supported by grants from the Swiss National Science Foundation, the Artères Foundation, the Astellas European Foundation, the Boninchi Foundation and the Association for Research in Surgery (ARS). Christian Toso was supported by a Professorship from the Swiss National Science Foundation (PP00P3_139021).

Conflict of interest

The authors who have taken part in this study declared that they do not have anything to disclose regarding funding or conflict of interest with respect to this manuscript.

Acknowledgement

The authors would like to thank Wolfgang Wirth of PMU, Austria, for providing the segmentation software.

Supplementary data

Supplementary data associated with this article can be found, in the online version, at http://dx.doi.org/10.1016/j.jhep.2014.03.036.

References

[1] Grewal HP, Willingham DL, Nguyen J, et al. Liver transplantation using controlled donation after cardiac death donors: an analysis of a large single-center experience. Liver Transpl 2009;15:1028–1035.

[2] Hernandez-Alejandro R, Croome KP, Quan D, et al. Increased risk of severe recurrence of hepatitis C virus in liver transplant recipients of donation after cardiac death allografts. Transplantation 2011;92:686–689.

[3] DeOliveira ML, Jassem W, Valente R, et al. Biliary complications after liver transplantation using grafts from donors after cardiac death: results from a matched control study in a single large volume center. Ann Surg 2011;254:716–722, [Discussion 722–723].

[4] Fondevila C, Hessheimer AJ, Flores E, et al. Applicability and results of Maastricht type 2 donation after cardiac death liver transplantation. Am J Transplant 2012;12:162–170.

[5] Abt PL, Desai NM, Crawford MD, et al. Survival following liver transplantation from non-heart-beating donors. Ann Surg 2004;239:87.

[6] van der Bilt JDW, Kranenburg O, Nijkamp MW, et al. Ischemia/reperfusion accelerates the outgrowth of hepatic micrometastases in a highly standardized murine model. Hepatology 2005;42:165–175.

[7] Ku Y, Kusunoki N, Shiotani M, et al. Stimulation of haematogenous liver metastases by ischaemia-reperfusion in rats. Eur J Surg 2003;165:801–807.

[8] Toso C, Mentha G, Majno P. Liver transplantation for hepatocellular carcinoma: five steps to prevent recurrence. Am J Transplant 2011;11:2031–2035.

[9] Oldani G, Lacotte S, Morel P, et al. Orthotopic liver transplantation in rats. J Visualized Exp 2012;65:e4143.
[10] Oldani G, Maestri M, Gaspari A, et al. A novel technique for rat liver transplantation using Quick Linker system: a preliminary result. J Surg Res 2008;149:303–309.
[11] Luetteke NC, Michalopoulos GK, Teixido J, Gilmore R, Massague J, Lee DC. Characterization of high molecular weight transforming growth factor alpha produced by rat hepatocellular carcinoma cells. Biochemistry 1988;27:6487–6494.
[12] Lesurtel M, Soll C, Humar B, Clavien PA. Serotonin: a double-edged sword for the liver? Surgeon 2012;10:107–113.
[13] Soll C, Jang JH, Riener M, et al. Serotonin promotes tumor growth in human hepatocellular cancer. Hepatology 2009;51:1244–1254.
[14] Lonati C, Sordi A, Giuliani D, et al. Molecular changes induced in rat liver by hemorrhage and effects of melanocortin treatment. Anesthesiology 2012;116:692–700.
[15] Muth M, Theophile K, Hussein K, Jacobi C, Kreipe H, Bock O. Hypoxia-induced down-regulation of microRNA-449a/b impairs control over targeted SERPINE1 (PAI-1) mRNA-a mechanism involved in SERPINE1 (PAI-1) over-expression. J Transl Med 2010;8:33.
[16] Zhang Y, Furuyama K, Kaneko K, et al. Hypoxia reduces the expression of heme oxygenase-2 in various types of human cell lines. A possible strategy for the maintenance of intracellular heme level. FEBS J 2006;273:3136–3147.
[17] Tolboom H, Pouw RE, Izamis ML, et al. Recovery of warm ischemic rat liver grafts by normothermic extracorporeal perfusion. Transplantation 2009;87:170–177.
[18] Perk S, Izamis ML, Tolboom H, et al. A metabolic index of ischemic injury for perfusion-recovery of cadaveric rat livers. PLoS One 2011;6:e28518.
[19] Schlegel A, Rougemont O, Graf R, Clavien PA, Dutkowski P. Protective mechanisms of end-ischemic cold machine perfusion in DCD liver grafts. J Hepatol 2013;58:278–286.
[20] de Rougemont O, Breitenstein S, Leskosek B, et al. One hour hypothermic oxygenated perfusion (HOPE) protects nonviable liver allografts donated after cardiac death. Ann Surg 2009;250:674–683.
[21] Henry SD, Nachber E, Tulipan J, et al. Hypothermic machine preservation reduces molecular markers of ischemia/reperfusion injury in human liver transplantation. Am J Transplant 2012;12:2477–2486.
[22] Vogel T, Brockmann JG, Friend PJ. Ex-vivo normothermic liver perfusion: an update. Curr Opin Organ Transplant 2010;15:167.
[23] Sass G, Leukel P, Schmitz V, et al. Inhibition of heme oxygenase 1 expression by small interfering RNA decreases orthotopic tumor growth in livers of mice. Int J Cancer 2008;123:1269–1277.
[24] Tanaka S, Akaike T, Fang J, et al. Antiapoptotic effect of haem oxygenase-1 induced by nitric oxide in experimental solid tumour. Br J Cancer 2003;88:902–909.
[25] Zou C, Zhang H, Li Q, et al. Heme oxygenase-1: a molecular brake on hepatocellular carcinoma cell migration. Carcinogenesis 2011;32:1840–1848.
[26] Nath B, Szabo G. Hypoxia and hypoxia inducible factors: diverse roles in liver diseases. Hepatology 2012;55:622–633.
[27] Greenberger LM, Horak ID, Filpula D, et al. A RNA antagonist of hypoxia-inducible factor-1alpha, EZN-2968, inhibits tumor cell growth. Mol Cancer Ther 2008;7:3598–3608.
[28] Weng CJ, Tsai CM, Chen YC, et al. Evaluation of the association of urokinase plasminogen activator system gene polymorphisms with susceptibility and pathological development of hepatocellular carcinoma. Ann Surg Oncol 2010;17:3394–3401.
[29] Grivennikov SI, Greten FR, Karin M. Immunity, inflammation, and cancer. Cell 2010;140:883–899.
[30] Park EJ, Lee JH, Yu G-Y, et al. Dietary and genetic obesity promote liver inflammation and tumorigenesis by enhancing IL-6 and TNF expression. Cell 2010;140:197–208.
[31] Zuo Y, Ren S, Wang M, et al. Novel roles of liver sinusoidal endothelial cell lectin in colon carcinoma cell adhesion, migration and in-vivo metastasis to the liver. Gut 2013;62:1169–1178.
[32] Li CX, Shao Y, Ng KTP, et al. FTY720 suppresses liver tumor metastasis by reducing the population of circulating endothelial progenitor cells. PLoS one 2012;7:e32380.
[33] Jay C, Ladner D, Wang E, et al. A comprehensive risk assessment of mortality following donation after cardiac death liver transplant – An analysis of the national registry. J Hepatol 2011;55:808–813.